Application of an Integrated Blowout Model System, OILMAP DEEP, to the Deepwater Horizon (DWH) Spill

Malcolm Spaulding[1], Zhengkai Li[2, 3], Daniel Mendelsohn[2], Deborah Crowley[2], Deborah French-McCay[2], and Andrew Bird[2]

[1] Ocean Engineering, University of Rhode Island, Narragansett, RI 02882, U.S.A.,
[2] RPS ASA, South Kingstown, RI 02879, U.S.A.
[3] PureLine Treatment Systems, Chicago, IL 60106, U.S.A.

Abstract

OILMAP DEEP, an integrated system of models (pipeline release, blowout plume, dispersant treatment, oil droplet size distribution, and fountain and intrusion), was applied to the Deepwater Horizon (DWH) oil spill to predict the near field transport and fate of the oil and gas released into the northeastern Gulf of Mexico. The model included multiple, time dependent releases from both the kink and riser, with the observed subsurface dispersant treatment, that characterized the DWH spill and response. The blowout model predictions are in good agreement with the available observations for plume trapping height and the major characteristics of the intrusion layer. Predictions of the droplet size distribution are in good agreement with the limited *in situ* Holocam observations. Model predictions of the percentage of oil retained in the intrusion layer are consistent with independent estimates based on field observations.

Keywords: blowout modeling, blowout plume dynamics, plume trapping and intrusion, oil droplet size distribution, subsurface dispersant treatment, pipeline flow modeling

1. Introduction

The Deepwater Horizon (DWH) spill, the largest offshore oil blowout in history, represents an unprecedented opportunity to evaluate the performance of state of the art blowout models to predict the dynamics of the release, including the effects of dispersant treatment on the spill. The spill began on April 20, 2010 and ended on July 15, 2010 (87 days). Based on government estimates (Lehr et al. 2010) a total of approximately 4.11 million barrels was released to the environment, with a typical release rate of 50,000 to 60,000 barrels per day.[1]The release occurred off the southern coast of Louisiana in a water depth of about 1500 m. The release was initially from a series of small holes at a kink in the rise pipe above the blowout preventer (BOP) and at the end of the riser pipe. The riser pipe was cut above the BOP on June 3, 2010 and oil was recovered via a top hat placed above the BOP from this date until the well was shut in on July 15, 2010. Dispersants were applied to the release from riser at the rate of about 200- 300 barrels per day from late April to well close in. This is the first time that dispersants have been applied to a major blowout.

Socolofsky et al. (2011) applied their empirical method to predict the trap height for the DWH spill and compared model predictions to observations based on fluorescence measurements of Colored Dissolved Organic Matter (CDOM) concentrations. Model predictions were in good agreement with the observations, correctly predicting the mean trap height but did not address the multiple releases from the riser and kink. No predictions of oil droplet size distribution or the impacts of dispersant treatment on the release were presented in this paper.

1. Note that while in January 2015, the U.S. District Court for Eastern District of Louisiana (Case 2:10-md-02179-CJB-SS Document 14021 Filed 01/15/15 (USDC 2015)) found that 3.19 million

barrels of oil were released to the water column, analyses herein were based on the government's estimate.

The objective of this paper is to provide a very brief overview of the integrated deep water oil and gas blowout model system (OILMAP DEEP) and then describe its application and validation to the near field fate and transport processes of the DWH spill. The model predicts the oil and gas release from the pipeline, the blowout plume associated with the discharge and its trapping depths, the dissolution of gas from the rising plume into the water column, the oil droplet size distribution, the fraction of oil treated with a specified application method and the associated dispersant-to-oil ratio (DOR), and the characteristics of the fountain and intrusion layer on a daily basis. The model addresses both chemically treated (by dispersant) and untreated oil from single- and multiple-point time-varying sources. The model spatial scales extend from tens to hundreds of meters above the seabed and within hundreds of meters to a km horizontally from the blowout location, while its temporal scale extends over the duration of the release. More detailed information on the effort is provided in Spaulding et al. (2015). Section 2 gives an overview of the integrated blowout model including pipeline release, blowout plume, dispersant treatment, oil droplet, and fountain/intrusion model components. Far field transport and fate of the oil was simulated using SIMAP and validated with available observations of oil in the water column and at the surface (French McCay et al., 2017). Section 3 provides a specification of the environmental conditions during the spill, the amount of oil released and dispersant applied, and then presents the application and validation of the model to the DWH spill by model component. Predictions of the amount of oil that remains in the deep water for various treatment strategies, using the dispersant treatment and oil droplet size models, are provided in Section 4. Section 5 provides summary and conclusions and references are given in Section 6.

2. Overview of OILMAP DEEP and Model Components

OILMAP DEEP is comprised of five integrated model components (pipeline release, blowout plume, dispersant treatment, oil droplet size, and fountain and intrusion) that are assembled to predict the dynamics of the release of oil and gas to the water column from a subsea blowout, with and without subsurface dispersant treatment. The integrated system is primarily focused on predicting the dynamics of the plume and resulting intrusion layer, the dissolution of gas, formation of hydrates, and the oil droplet size distribution and concentrations. Figure 1 shows a schematic of the system with ovals representing individual model components and the boxes, data inputs. As a conservative assumption, oil droplets are assumed not to undergo dissolution or biodegradation within the blowout plume given the fast rise times. These processes are however included in the far field transport, fate, and effects model (SIMAP) (French McCay et al., 2015, 2016) (not discussed here).

The pipeline release model predicts the release rate of oil and gas from various openings in a riser pipe system. The blowout plume model predicts the characteristics of the plume resulting from the oil and gas release including its orientation, radius, velocity, entrainment rate, and oil and gas concentrations as a function of distance from the release location and the trapping height/depth (height is measured from the release location near sea floor and depth from the water surface). The trapping depth is the location where plume buoyancy is lost by entrainment of ambient seawater and gas dissolution, which results in rapid radial spreading of the plume into an intrusion layer. The trapping height/depth is defined at the center of the intrusion layer. The dispersant treatment model predicts the fraction of oil treated and the effective dispersant to oil ratio (DOR) for the specified application method and amount of dispersant applied. The oil droplet size model predicts the oil droplet size distribution, with and without dispersant treatment, for single or multiple release locations. The fountain and intrusion model predicts the geometry (height and thickness versus distance) of the fountain formed above the trap depth and the associated flow intrusion observed at the trap depth. Additional details on the model framework are provided in the supplemental material.

Predictions of the blowout plume model (trapping height and plume diameter for each release), and the oil droplet size model (volume-weighted oil droplet size distribution, with or without dispersant treatment), are provided as input to SIMAP (far field fate and transport model). Predictions from the fountain and intrusion model (peak height at release, flow rate and thickness of the intrusion layer as a function of distance from the source) are also available for finer scale evaluations in the area in the immediate vicinity of the wellhead. The blowout and droplet size model simulations are normally performed on a daily time step which matches the temporal resolution of the input data for the oil release and subsurface dispersant application rates.

3. Application of OILMAP DEEP to DWH Spill

Environmental Conditions

To establish the environmental setting for model application, information on the receiving water density structure and current was reviewed. Both variables play a central role in blowout modeling. The degree of vertical stratification in the water column has an important influence on the plume trapping depth, while the currents affect the behavior of the plume and whether it bends over allowing gas bubbles to escape, which can deprive the plume of one of its sources of buoyancy.

A review of the CTD (Conductivity, Temperature, and Depth) measurements made in the vicinity of the DWH spill site between April and November, 2010 (Grennan et al. 2015) was performed and shows that the variability in density decreases rapidly with depth; with high variability in the surface layer (to a depth of 200 m) (Figure S1). In the depth range of interest (trap depth and intrusion layer) for the DWH release (depths of 900 to 1,300 m), there is little variation in the vertical structure of the density profile or its values, suggesting that a constant density gradient structure in the vicinity of the trapping depth, over the duration of the spill, is a reasonable approximation.

Two Acoustic Doppler Current Profilers (ADCPs) were deployed in the vicinity of the wellhead from early May through the end of July 2010. The mean current speed values (and their variances) at the depth bin (depth interval) closest to the trapping height of the plume (~900 m below surface) of the two ADCPs were 6.7 ± 4.7 and 6.9 ± 5.2 cm/sec, respectively. The magnitude of the deep water currents hence was quite low and variable and therefore would not have a substantial impact on plume behavior (e.g. plume bending).

Oil release rate

Estimates of the oil release rate were initially presented in the NOAA Oil Budget Calculator (OBC) (Lehr et al., 2010) based on analyses of the Flow Rate Technical Group (FRTG) (McNutt et al. 2011), which gave a mean value of 4.94 million barrels over the 87 day release period from April 22 to July 15, 2010. The US Department of Justice (DOJ) subsequently contracted with five experts (Bushnell 2013; Pooladi-Darvish 2013, Dykhuizen 2013; Griffith 2013; Kelkar and Raghavan 2013) to provide estimates of the flow rate vs time and the total release from the DWH spill (Figure S2). Each expert made estimates, using their selected methodology, for discrete time periods during the release, and for the total release, along with the associated uncertainties. An additional report was prepared by Zick (2013) to characterize the oil and gas mixture and provide it in the form of an equation of state, as a function of pressure and temperature (Black Oil Tables, BOT).

The results of the DOJ experts are in very good agreement with the OBC estimates for mean values (DOJ experts- 4.96 million barrels vs OBC- 4.94 million barrels). The uncertainties for the DOJ estimates are slightly larger (6 to 7%) than those from the OBC (4 %). The temporal trends in release rates are very similar between the two. Given the very good agreement between the results of the various experts and the OBC estimates, the OBC values were selected for the present application.

Figure 2 shows the time history of the oil release rate to the water column from April 22, 2010 to July 15, 2010 based on the OBC report (Lehr et al. 2010. Based on the OBC (in solid black line), the release rate decreased from just over 60,000 barrels per day at the start of the spill to about 55,000 barrels per day by the time the release stopped. Estimates of the amount of oil recovered are also provided. Oil was released in one of two different configurations. The first (prior to June 3) had varying percentages of the total released from two primary locations, one at the end of the riser and the other from a number of small holes in the vicinity of a kink that developed in the riser pipe, immediately above the BOP. The second configuration reflected flow only after the riser pipe was cut immediately above the BOP on June 3, 2010. The discrete stepping of the kink release is a result of the increase in the number of holes at the kink. The estimates of each flow rate were based on the application of the pipeline model, described below, using the gas-to-oil ratios (GOR) and densities estimated at the surface and at depth conditions as provided in Zick (2013), and information on the kink-hole geometries provided by the USCG (2010).

Specification of dispersant application strategy and amount applied.

A review of Remotely Operated Vehicle (ROV) video taken during the release (Spaulding et al, 2015) showed that dispersants were applied by a variety of applicators to the riser release. Figure 3 identifies five dispersant applicator types (hook, paddle, collar, trident, and wand) over the duration of application. Two devices were primarily used: a wand and a trident (bi-dent or forked wand) (Figure S3). In both methods, the applicator was typically placed adjacent to the oil release and the dispersant entrained into the plume/jet as it exited the riser. No dispersant treatment was applied at the kink. ROV video suggests that a wand was used to apply dispersants at the end of the riser pipe before it was cut, and that the trident was predominantly used post-riser cut while the top-hat was in place. Even though the wand and trident were the applicator types used predominantly throughout the spill, other application methods and combined methods were also utilized. The time history of the amount of dispersants applied is provided in the OBC report and shown in Figure 2. The nominal application rate, based on EPA guidance, was approximately 10 gpm.

Presented below are the results of the application of the various components of the model, by individual model. An overview of model processes, formulation, inputs, and outputs is provided in the supplemental material section, with full details in Spaulding et al. (2015).

Pipeline release model

On April 28, 2010, the riser pipe just above the BlowOut Preventer (BOP) began to leak at a point where the pipe had been severely kinked during the riser collapse. Between April 28 and June 3, 2010, the number of holes in the kink area increased from the initial two up to six holes (Figure S4). As the release continued, the holes in the kinked riser increased in size and number, and released a large amount of oil and gas that might otherwise have travelled the length of the riser to the severed end of the pipe several hundred meters away. The oil and gas released through the kink holes was under considerable pressure and was forced through fairly small holes, creating high velocity oil and gas jets. The exiting oil/gas mixture was therefore driven by far greater energy than if it had exited from the much larger riser pipe outlet. The increased energy has the effect of shifting the droplet size distribution to smaller sizes, many more of which could become trapped in the lower water column, changing the oil mass balance between the oil mass surfacing and that remaining at depth. In addition, the amount of oil and gas released affects how the plume of released material behaves in the water column, as it rises due to buoyancy, entraining surrounding waters and finally trapping at some height above the blowout.

The pipeline release model was employed to determine the flow distribution split between the kink holes and the riser outlet. Inputs to the model on the oil characteristics were obtained from Black Oil Tables (Zick ,2013), riser geometry and kink holes from BP and US Coast Guard (USCG, 2011), and pressure in the riser pipe from the FRTG (McNutt et al, 2011). Use of the BOT allowed a complete characterization of oil and gas density and viscosity at the depths (pressure) and temperature of the release.

Simulations were performed with pipeline release model from April 28 through June 2, 2010 to predict the daily flow balance between the riser and the kink flows. The riser was cut above the BOP on June 3. Figure 4 presents the model predicted kink and riser flow rates and the total flow from the well, as a function of time, over that period; note that these values do not take into account any of the release that was collected, since this occurs after the release and therefore does not impact the pipeline flow distribution analysis. The predicted amount of oil released from the kink was on the order of 11,000 bbl on the first day, increasing to 16,000 bbl immediately before the riser was cut, equating to 18% of the total amount initially released, and increasing to 28% at the end.

While the blowout was still in progress, investigators made estimates of the amount of oil leaking from the kink area. Estimates were made by members of the FRTG using Particle Image Velocimetry (PIV) (McNutt et al. 2011) for May 15, 2010, prior to the formation of the FRTG (Wereley 2011), and estimated the kink flow at 35% of the riser flow, which corresponds to 26% of the total flow. Additional estimates were made using PIV methods after the formation of the FRTG and gave values ranging from 15 to 20% for May 14-16, 2010. Camilli et al. (2011) estimated the flow split, based on ADCP measurements for May 31, 2010, and gave a value of 31%. The estimates, for May 14-16, correspond to the time when only two holes were in existence, whereas by May 31, all six holes were present. The model predictions are in generally good agreement with the observations, both in terms of the percentage of oil released at the kink and its temporal trend.

Dispersant treatment model

The dispersant treatment model was developed based on estimating the dilution factor of the entrainment of ambient seawater, and the initial and growing fraction of the cross section of the plume where active mixing of the released oil and the applied chemical dispersants occurred. This approach is based on the observation that in most cases dispersants were applied at the edge of the jet/plume and entrained into the rising plume (Figure S3). The dilution factor is determined by assuming either a momentum jet or a buoyant plume flow, depending on the distance of dispersant application relative to the jet/plume transition length scale. The fraction of the treated cross section of the plume is determined by the dispersant application device; a trident application results in a wider contact angle of dispersant with the plume than a wand (Figure S3), and therefore the fraction treated is proportionally larger with the trident compared to the wand application.

The dispersant treatment model was applied to the DWH spill. As a first step, the momentum length scale was calculated for the pre- and post-cut riser releases. This calculation was performed to determine the length scale at which the flow regime changes from a jet to a plume, based on the ratio of the momentum to buoyancy of the release. This distinction is of key importance to choosing the proper analytical solution for the entrainment calculations. The calculated length scale for the riser ranged from 0.5 to 0.8 m, depending on the assumption about the flow rate and release opening geometry. Estimates were also made for the kink release and gave values of 3 to 5 m, depending on the number of holes and the associated flow rates. Camilli et al. (2011) gave estimates of the momentum length scale for the pre-cut riser of 0.6 m for May 31, 2010, in very good agreement with the analysis presented here. Estimates of the length scale for the kink release are not of concern here since no dispersants were applied at this location. Based on this analysis and the observation from the ROV imagery, that the dispersants were typically applied near the end of the riser and that entrainment and subsequent mixing proceeded with distance from the release point, it is reasonable to assume that the release can be best approximated as a buoyant plume, with the buoyancy of the oil and gas driving the plume.

To assess the model's predictive performance, it was applied to predict the fraction treated and DOR during the time period when oil droplet sizes were being measured by Holocam during various dives from the R/V Jack Fritz 3 cruises (Davis and Loomis, 2014). During this period, dispersants were primarily being applied via the trident immediately above the release and in close proximity to the mouth of the top hat. Dispersant treatment model simulations were performed for June 14 to 20, 2010, with a time step of one day. Daily oil release and dispersant application rates were used.

Figure 5 shows model predictions of fraction treated and DOR as a function of time assuming 20, 30, and 40% of the angular sector was treated. The 30% value is a reasonable estimate for the trident. The results are shown at approximately six (6) pipe diameters from the release origin. The model predicts percent treated of 16, 25, and 34% (solid lines) for the 20, 30, and 40% sector cases, respectively. These percent treated values are invariant with time. The DOR for each sector case is also shown (blocks, right axis) and varies daily throughout the period; the higher the percent of sector treated, the lower the DOR. The day-to-day variations are caused by changes in the oil release and dispersant application rates, leading to a wide range of the ratios of daily oil flow to dispersant flow rates (92 to 242). Fraction treated and DOR both scale linearly with the percent of sector. The average DORs during the period are 1:33, 1:49, and 1:65 for the 20, 30, and 40% cases, respectively.

The DORs for R/V Jack Fritz dives #5 and #6, where Holocam data were collected, were estimated using the droplet size model. Far field simulations using SIMAP (French McCay et al, 2017) showed that droplets being measured during these dives were the result of recent releases and not the remnants of small droplets trapped at the intrusion layer from earlier releases. Specifically, an assumed lognormal distribution was fit to the observations from each dive and the volume median diameter (VMD) determined for each. The equation that expresses VMD as a function of Weber (We) and Ohnesorge (Oh) number was then used to estimate the most likely value of the oil-water interfacial tension associated with the observed VMD. This value in turn was used to determine the DOR based on laboratory based observations of DOR vs oil water interfacial tension for Macondo oil and Corexit 9500 dispersant (Venkataraman et al. 2013).

Venkataraman et al (2013) curves were selected for the DWH simulations as it was generated from fresh source oil MC252 oil and Corexit 9500 dispersant and hence most closely matched the conditions for subsurface dispersant applications during the spill that were available at the time this work was performed.

The modeled DORs for dives #5 and #6 are shown in Figure 5. The value to the right of the dive number is the horizontal distance (m) between the sampling site and the wellhead. The Holocam data-based DOR of 1:69 and 1:114.5, were estimated for dives #5 and #6, respectively. Model prediction for dive #5 are in good agreement with the very limited observations. The maximum depth of dive #6 is only 1059 m and hence may have not fully reached the trapped intrusion layer. It is therefore likely that not all of the small droplets have been fully measured and hence explains why the back-calculated apparent DOR is higher than model predictions.

The dispersant treatment model predicts a variation in the DOR with time, which is in general agreement with the overall trend of the observational data. The variation of field data is not surprising, given the quite different distances (at locations ranging from approximately 1.15-2.12 km from the wellhead) and direction (oriented north to northwest from the wellhead) associated travel time of oil droplets from the source to the sampling location prior to when the Holocam based observations were made. As the droplet size data were collected at a distance from the wellhead, they may not include the portion of the release that was in the form of larger droplets, which could have reached the surface before being sampled.

Blowout plume model

The blowout plume model was applied to simulate the release of oil and gas from subsurface release location(s) to predict subsurface plume size and location, as well as the concentration of oil and gas along the plume centerline. The model predictions are largely dependent on the relative density difference between the release and the receiving water; this density difference (buoyant force) causes the plume to ascend vertically and while doing so, entrain water and spread radially. This entrained water mixes with the release resulting in the dilution of the plume oil and gas concentrations, while also slowing the plume ascent and rate of entrainment. The model also simulates the dissolution of gas from bubbles into the entrained water, which also serves to reduce the plume buoyancy. These actions combine to eventually "trap" the plume, meaning the plume (mixture of the oil and gas release with water) eventually reaches a state of neutral buoyancy and no longer ascends through the water column. At this point, the ascent of the oil droplets is a function only of their individual buoyancy driven rise velocity (a function of size and density).

Independent simulations were performed on a daily basis for both the riser and kink releases. Ambient water column stratification was obtained from Grennan et al. (2012), oil and gas properties from Zick (2013), and release rates from OBC, as shown in Figure 2.

Figure 6 illustrates the model-predicted plume radius and centerline velocity as a function of height above the release for representative days. Included on the plot are the predictions from both pre-cut (35,000 bbls/day) and post-cut riser (47,000 bbl/day) on a day with average flow conditions, as well as the kink flow for initial (13,000 bbl/day) and final flow conditions (19,000 bbl/day). In all cases the centerline velocity decreases and the plume radius increases with increasing height. This figure shows that the predicted plume centerline velocity is typically between 0.7-0.8 m/s initially and decreases with increasing height, while the initial kink plume centerline velocity is between 0.5-0.6 m/s. Conversely, the model predicts that the plume radius is initially approximately 10 m for both the kink and riser and gradually increases to approximately 90 m for the riser release and approximately 65 m for the kink at trap height. The initial 10 m plume radius is a result of the initialization process of the plume integral equations. The plume model does not explicitly solve the momentum jet (where momentum forces dominate buoyant forces) and transition to the buoyant plume, but rather initializes the solution based on the physical and numerical properties of a fully developed buoyant plume at a small distance above the plume source.

The model predicted trap heights were compared to observations of excess CDOM in the water column. The CDOM anomaly, characterized by water samples that had greater than 1.5 times the background fluorescence levels, indicates the presence of hydrocarbons from the trapped plume. A series of example excess CDOM vertical profiles, taken in the region of the well, is presented in Figure S5. Figure 7 illustrates model predictions of trap height versus the excess CDOM observations for the period of the blowout. The observations in this figure represent the upper and lower height bounds of excess CDOM taken from locations close to the wellhead and with sufficient number of samples, as well as the depth of the maximum excess CDOM measured in the profile. Details regarding the background CDOM levels, data analysis, and results are documented in Horn et al. (2015).

As clearly shown in Figure 7, the model predicted trap height from the riser release varied from 359 to 299 m from the sea floor (or 1150 to1210 m below the surface), while values for kink release were 234 to 199 m from the sea floor (or from 1275 to 1310 m below the surface). These predictions compare well with the excess CDOM anomaly, which was observed between approximately 800-1300 m below the surface, with the peak excess CDOM anomaly observed mainly between 1100-1300 m below the surface. The model was able to capture the differing trends between the two releases, as seen with the predicted trap height from the kink lower than that from the riser.

Spier et al. (2013) performed an investigation of the distribution and chemical composition of hydrocarbons released from blowout using available hydrocarbon data acquired from NOAA and BP. The analysis identified a deep water plume of hydrocarbons centered at 1175 m below the surface. This analysis is consistent with the CDOM data presented here and with plume model predictions of trapping heights (Figure 7). In addition, Spier et al. (2013) also observed oil at other depths such as 865 m and 265m, but it is likely not fresh oil but remnants of earlier releases after loss by dissolution of the more soluble fractions, as evidenced by the differing weathering states of the measured hydrocarbons (Payne and Driskell, 2015a,b; Horn et al., 2015; French McCay et al., 2016).

The blowout model formulation includes gas dissolution. In this application the gas is assumed to be primarily methane (Reddy et al, 2012). The rate of dissolution is primarily a function of the amount of gas in the release and the initial gas bubble size associated with the release. As the gas dissolves, it reduces the plume buoyancy and increases the dissolved methane concentration in the plume water. The model predicted the plume gas volume and the methane concentration along the plume centerline for the riser and the kink (Figure S6). Based on the model predictions, it is anticipated that dissolved methane in the plume water would be found above the release up to a vertical extent of approximately 350 m, or approximately 1,150 m below the surface, and hence the trap depth.

The model predicted dissolution of methane into the water column is in good agreement with the findings with Kessler et al. (2011) who investigated the dissolved oxygen anomaly during the spill. This study reported observations of high water column concentrations of methane at depths between 800 - 1,200 m. Reddy et al. (2012) suggested that the methane gas in the blowout plume had completely dissolved (99.99%) by the time it trapped, at approximately 1,100 m depth level. These findings are also reflected in the blowout plume model predictions of methane gas dissolution, as shown in Figure S6, namely that all the gas has dissolved by the time the plume reaches a height of 350 m above the bottom.

The blowout plume model formulation includes the ability to model the formation and dissolution of methane hydrates. While the temperature and pressure regime at the release sites was sufficient for potential hydrate formation (Anderson et al., 2012), the methane concentration in the water column was found to be too low to support stable hydrate formation.

Droplet size model

A new, unified, empirically-based oil droplet size model, dependent on both the Weber (We) and Ohnesorge (Oh) numbers (Hinze 1955) was used to determine the Volume Median Diameter of droplet size (VMD). The model assumes that the droplets are log-normally distributed and addresses the impact of dispersant treatment through changes in oil water interfacial tension on the Oh number. The model development and application are described in detail in Li et al. (2016) and Spaulding et al. (2015). The model parameters were calibrated with data from the DeepSpill experiment (Johansen et al. 2001), grid column experiments for low and moderate viscosity oils (Delvigne and Sweeney,1988; Delvigne and Hulsen 1994), and wave tank breaking wave experiments for more viscous oils (Reed et al., 2009). The model was then validated against several small and large scale laboratory studies on subsurface releases of oil, with and without dispersant treatment (Brandvik et al. 2014 and Belore 2014).

The model was used to estimate the droplet size distributions from the various releases (kink, and pre- and post- riser cut). The droplet model predicted that the VMD from the untreated riser flow changed from 2,300 µm prior to the riser cut, to 3,000 µm during the kink flow period, and finally to 2,700 µm after the riser cut. Simulations of the kink release showed that the VMD ranged from 330-360 µm. The large difference between the riser and kink droplet sizes is a result of the differential flow velocity between the riser flow, with a relatively large cross sectional area, and the kink flow, with multiple holes with much smaller cross sectional areas. The variability in the riser droplet sizes was due to differences in flow rate; smaller sizes corresponding to higher flow rates. The release from the kink had less variability in the exit velocity and therefore a smaller range of median droplet sizes.

In the presence of dispersant treatment, the model predicts reduced droplet sizes. The treated oil at the riser is predicted to have much smaller droplet sizes than the untreated oil. The fraction of oil treated is dependent on the application method and the amount and effectiveness of dispersant treatment. The droplet size distribution of the total release is the volume-weighed distributions of treated and untreated oil. It has not been possible to verify all of the estimates of droplet sizes from the different sources and different treatments, given the fact that no droplet size data is available in the immediate vicinity of either the riser or kink releases.

To gain insight into the droplet size distribution, the dispersant and droplet size models were applied to predict the distributions observed from the Holocam measurements made during the M/V Jack Fitz 3 (JF3) cruise (June 14 to 20, 2010) (Davis and Loomis, 2014). The droplet size measurements were made during nine dives, with the maximum depths ranging from approximately 260 to 1490 m below the sea surface and distances of 1.15 – 9.32 km from the well head. The automatic processing data from each dive, (and only particles that were identified as class 1 (i.e., oil droplets)), were binned into discrete depth intervals of 100 m each for analysis. The data set was further restricted to dives where manual methods confirmed the results of the automated method and showed significant oil. Dispersants were being applied adjacent to the top hat during this post cut period by the trident, and hence the observed droplet size distribution is a result of both treated and untreated oil droplets.

Simulations were performed assuming DORs of 1:40, 1:90, 1:100, and 1:150, with fraction treated ranging from 0 to 100%. These values were selected to range the likely DORs since there is no direct way to measure them. The first two values represent DOR cases explored in the Oil Budget Calculator (Lehr et al. 2010) and 1:150 is representative of the approximate average value assuming all oil is treated for the JF-3 cruise period. Given the dispersants that were available, and assuming a complete (100%) effectiveness, these DORs imply that 26.5% (1:40), 60% (1:90), 67% (1:100), and 100% (1:150) of the oil would have been treated. Note these high treatment fractions (≥ 60%) are much greater than the treated fraction predicted in the dispersant treatment model. These values are controlled by the amount of dispersant available. For the oil that was treated it was assumed that the dispersant effectiveness was 100% (namely that the dispersant was completely mixed with the treated oil). Figure 8 (upper panel) shows the model-predicted droplet size distribution for values of DOR ranging from 1:40 to 1:150, model-predicted distribution assuming no dispersant effectiveness, and the droplet size distribution data observed from the JF3 field measurements (dives #5 and 6). The lower panel shows the same data but focusing on the distribution of droplets that are 300 μm or smaller. The modeled distributions are recalculated to be cumulative up to 300 μm. This droplet size range (0 to 300 μm) should reflect the droplets observed by the holocam at the distances of deployment from the source (see upper panel insert, right side for dive locations). Droplets larger than this size are predicted to have risen out of the trapped intrusion layer before reaching the dive locations at ~1 km from the source, given the mean current speed of 4 cm/s as measured by Acoustic Doppler Current Profilers (ADCPs) at the wellhead and a rise rate of 26 m/hr for a 300 μm droplet of light crude oil. As shown in Figure 8 (lower panel), model predictions below 300 μm are in reasonable agreement with the holocam observations. Figure 8 (upper panel) shows that a DOR of 1:40 predicts a smaller fraction of oil droplets matching the majority of the size distributions from the field observations, than those at a DOR of 1:90 and 1:100. A DOR of 1:150 and no dispersant treatment condition result in most oil droplet sizes larger than those observed in the field. When the model distributions are recast as cumulative to 300 μm, the observations fall between the model predictions assuming 1:40 and 1:150, most closely aligned with 1:90 or 1:100. The no-dispersant model distribution is clearly outside the range of the observed data (Figure 8, upper panel), predicting droplets larger than 600 μm and most droplets greater than 1 mm in diameter, indicating that the subsea dispersant application was effective in dispersing oil into the water column. The range of VMD for the two dives (#5, 6) that were reported to have *much oil*, had volume median diameters ranging from 70 to 250 μm. The standard deviation of the lognormal distribution was 0.59 ± 0.08. This compares well to 0.51 ±0.09 used in the model, which was fit to the Norwegian Deep Spill data (Johansen et al. 2001).

The present analysis provides a reasonable upper bound to the size of oil droplets that are retained in the water column (≤ 300 μm) by the time Holocam sampling occurred. Larger size oil droplets are predicted to travel to the sea surface quite quickly due to their buoyancy and rapid rise rates. To the best of our knowledge, this is the first time that direct field evidence is available to show the effect of subsurface application of dispersant on reducing the droplet size distribution from field measurements. The evidence, however, is limited to only two JF3 dives (#5 and 6).

This upper bound value (≤ 300 μm) is consistent with the results of the lab study on the effects of droplet size on intrusion and subsequent transport of subsurface oil spills (Chan et al. 2014). These authors found that the particle spread increases rapidly as the normalized particle slip velocity becomes smaller for Type 1a* plume (see Figure 6 of Chan et al. 2014), in which the particles are transported within the intrusion layer. This suggests that small oil droplets, on the order of several hundred microns, will be more widely distributed in the water column, whereas larger droplets, on the order of millimeters, will have low spread and will rise to the surface within a close range of the wellhead.

Observed VMDs (70-250 μm) were substantially smaller than the model estimates for the untreated post riser cut release (~2,700 μm). Comparison of the model predicted size distributions for the post-cut riser released oil in Spaulding et al. (2015) shows that there is very little overlap of the sizes of the dispersant-treated vs untreated oil droplets. Simulations were performed with the droplet size model and show that the predicted distributions are in very good agreement with observations if the oil water interfacial tension was reduced, corresponding to those predicted by the dispersant treatment model over the field sampling period (June 14th to 20th, 2010).

After the study was completed and the paper on the droplet size model submitted for publication additional data became available to allow improvement of the model. The model was recalibrated and the results published in Li et al (2016). Material has been added to the supplementary material section of this paper to show the sensitivity of model predictions for conditions typical of the DWH release to earlier work and to the model developed by Johansen et al (2013).

Fountain and intrusion model

The fountain and intrusion model was applied to the release and predictions made on a daily basis to predict the intrusion layer flows in the presence of ambient currents. As an example assuming a fixed release rate of 62,000 barrels per day, the fountain and intrusion model predicted a peak thickness of 100 m above the trapping depth. The mean ambient currents were approximately 0.07 m/s. The intrusion flow rate predicted by the blowout model for the riser release, approximately 2,200 m^3/sec, was used as input to the fountain and intrusion model. The final stage of the intrusion model, including effects of the ambient current and entrainment from the resulting plane wake flow, predicted flow rates on the order of 7,000 m^3/sec immediately downstream (within several km) of the source (Figure S7). These values are consistent with estimates by Camilli et al. (2010) and Kujawinski et al. (2011). No field measurements were available that could fully resolve the flows and concentrations of the fountain or the intrusion layer. Model results are, however, broadly consistent with observed CDOM profiles taken during the spill and the results of empirical model predictions of the peel height (fountain peak) and intrusion flow rates by Socolofsky et al. (2011).

The fountain and intrusion model and associated intrusion calculations were used to determine the amount of BTEX (Benzene, Toluene, Ethylbezene, and o-, m-, and p-Xylene) and the dioctyl sodium sulfosuccinate (DOSS) component of the dispersant that was retained in the intrusion layer. These two compound groups (i.e., BTEX and DOSS) were selected for the analysis since both are expected to be associated with the intrusion layer (highly soluble and related to the application of dispersants to the spill) and be present in close proximity to the wellhead. Estimates of percentage retained in the intrusion layer were made by dividing the observed fluxes of these two chemicals in the intrusion layer (concentrations multiplied by volume flow rates) by the amounts (mass per time) released at the well head.

Based on data summarized by Horn et al. (2015), BTEX (represents about 1.9 % by weight of the MC252 source oil) concentrations measured during the spill, in the near field of the release (≤ 10s km), shows the largest values in the immediate vicinity of the trapping depth, with the highest concentrations in the range of 50 to 100 μg/l. The concentrations display strong variability in both space and time, but are systematically higher in pre-cut (mean value -103 μg/L), compared to post riser cut period (mean value – 51μg/L). Sampling during the pre-cut period was generally restricted to the SW of the well head, while samples collected during the post cut period provided coverage of the entire directional distribution. In addition, there were two sources during the pre-cut period (kink and riser) with two separate trapping depths and only one during the post cut period (from the riser). Given the lack of adequate directional sampling and issues in dealing with multiple sources during the pre-cut period, analysis of retention was restricted to the post-cut period only. Estimates were made using the observed post-cut BTEX data, within 6 km of the well head, and the predictions of the intrusion flows. It was estimated that 27% ± 5% of the released BTEX was in the intrusion layer. The upper and lower bounds represent the 95% confidence limits on the retention estimate. Similar estimates were made for DOSS, and predicted that 90% ± 23% of DOSS was in the intrusion layer. This is consistent with the idea that DOSS should be associated with the dispersed fraction of the oil and hence almost completely trapped in the intrusion layer. The DOSS analysis also supports the estimates of the volume flux used in the BTEX analysis.

4. Sensitivity of model predictions to dispersant treatment case studies

To understand the impact of the efficacy of dispersant treatment on the oil droplet size distribution, a number of individual simulation cases were performed using OILMAP DEEP. In all cases, the oil release and dispersant application rates were as specified in the OBC report (Figure 2). The relative amounts from the kink and riser, pre-riser cut, were obtained from the pipeline release model. The time step in the analysis was daily. In each case a variation of the dispersant treatment model was performed, as appropriate, to predict the amount of oil treated on a daily basis and the resulting dispersant to oil ratio (DOR). The droplet size model was then used to predict the size distributions for both treated and untreated releases, including riser and kink flow, and for both pre- and post- riser cut periods. Finally the volume weighting procedure was then used to estimate the total oil droplet size distribution for each case. The results are reported in the form of cumulative percent of oil, as a function of droplet diameter, for each individual component (i.e., the kink, the treated riser, and the untreated riser) of the release and the total release.

Simulation cases were performed to estimate the upper and lower bounds, in terms of the oil droplet size distribution, by varying the relative treatment effectiveness in the use of dispersants to treat the oil. Treatment effectiveness is used here to represent the amount of oil that is chemically treated by application of the dispersant. This value is provided by the user. Operational and hydrodynamic effectiveness of dispersant treatment are calculated by the dispersant treatment model (see Spaulding et al, 2015 for details on definitions for chemical, operational, and hydrodynamic efficiencies). The reference or base case assumes no dispersant treatment. The three different treatment cases are briefly described below. Low, best-estimate, and high dispersant application refer to the assumed level of success in the use of the dispersant in treating the oil. In all cases the amount of dispersant actually applied each day was used.

Low dispersant application. This case assumes that all of the dispersant was mixed with the riser flow remaining after collection, with a 50% treatment effectiveness.

Best estimate dispersant application. This case represents the best estimate of the application of dispersant to the riser release during the spill based on observations (e.g. by ROV) during the spill. In this case, the dispersant treatment model assumptions were: (1) the fraction treated was estimated at the end of the flow establishment zone; (2) dispersant (chemical) effectiveness of 80%; (3) the volume of oil treated for the DOR calculation (i.e., treatment effectiveness) was estimated for dispersant applied by single wand pre-riser cut and by trident (bi-dent) post-riser cut with a 29.5 (8.2%) and 108 (30%) degree (percent of total degrees) sector treated, respectively (see Spaulding et al, 2015 for details) at the exit of the riser; and (4) determination of which application method was employed was based on a review of ROV video.

High dispersant application. This case assumes that all of the dispersant was mixed with the riser flow remaining after collection with a 100% treatment effectiveness.

It is important in comparing the results of the three cases to note that the *low and high dispersant* treatment cases assumed that all of the oil released from the riser was treated with 50 and 100 % dispersant efficiency, respectively while the *best estimate* varied the fraction of oil treated based on the dispersant application history, all with a dispersant efficiency of 80%.

Figure S8 and associated supplemental material show the cumulative and individual oil volume droplet size distributions on two representative days, May 30, 2010 (upper panels) immediately before the riser was cut and June 10, 2010 (lower panels), shortly after it was cut. To give a sense of the mean conditions during the spill, Figure 9 shows plots of cumulative (upper panel) and individual (lower panel) droplet size distributions over the entire release period for each dispersant case. These were generated by weighting the daily values by the volumes released. The oil droplet size distributions are predicted to move to smaller sizes as a result of treatment; the more effective the dispersant treatment, the greater the shift to lower values. The effect of the riser cut and elimination of the kink as a source of smaller droplets is masked here since it is included in all cases.

In evaluating the results, it is useful to understand the impact of the droplet size on the droplet rise velocities. As a reference point, let us assume that droplets smaller than 300 μm, which take several days to rise to the surface, remain effectively trapped in the deep water while those larger than this size rise to the surface. This is consistent with analysis of the JF-3 data. This is also consistent with the results of the effect of droplet sizes on the intrusion and subsequent transport of oil droplets from a recent lab study by Chan et al. (2014).

Table 1 shows the cumulative volume oil droplet size distributions for the four cases. These data represent the mean values over the total release period and hence are the same values shown in Figure 9. For the untreated base case, using 300 μm as the reference point, most of the oil (91%) rises to the surface, with about 9% remaining in the deep water. As the level of dispersant treatment increases, the percent of oil at or below 300 μm increases with level of treatment: 11% for the low treatment level case, 22% for the best estimate, and 36% for the highest level of treatment. As dispersant treatment becomes more effective the oil droplet size distribution shifts to the left to smaller sizes (Figure 9).

To validate the model-predicted estimate of the fraction of the released oil that is dispersed in the water column, it would be ideal to have independent measurements made of the amount of oil in the water column. This of course was not possible given the problem of sampling total oil concentrations at depth over very large spatial and temporal scales. Some information is however available that can provide insight into the model performance evaluation.

Table 2 summarizes estimates of the percent of oil dispersed into the water from various sources and methods. Details are provided in Spaulding et al. (2015). The model predicted retained values are 11%, 22%, and 36% for low, best-estimate, and high dispersant effectiveness treatment cases (9 % for the untreated case). These values are consistent with estimates made based on the application of the plume and intrusion models using BTEX (27± 5%). The results are also consistent with the OBC, if estimates of the chemically and mechanically dispersed subsurface oil are used (20, 25, and 38%, least, expected, and most, respectively). The prediction is however lower than the estimates based on petroleum hydrocarbon (both oil and gas) chemistry data (low 28%, average 36%, high 45%; Ryerson et al., 2012). The average of all expected or best estimate value is 25.5 %, in reasonable agreement with the model predicted best estimate of 22%.

5. Summary and conclusions

OILMAP DEEP has been applied to the DWH spill to hindcast the release of oil and gas during the blowout into the water column. Comparisons between model predictions and observations have been made when data is available. The major conclusions of the study are as follows:

- The DWH release is significantly more complicated than what most blowout simulations have addressed: The release occurred from two separate locations (kink and riser) pre-riser cut and one location (riser) post-riser cut; the relative flow rates between the kink and riser varied with time as the number of holes and size of the openings at the kink increased with time, and the oil flow rates varied. The pipeline release model reasonably captured the relative flow rates between the two sources, pre-riser cut, based on BOT oil and gas properties and pipeline release system configurations; the predicted results are consistent with the observations of the releases using Particle Image Velocimetry (PIV) and Acoustic Doppler Current Profiler (ADCP) methods.

- The blowout plume model was used to predict the trapping height for both pre-cut riser and kink flow and the post-cut riser flow. As a result of the multiple sources and the varying flow rates, the model predicted three trapping depths; riser and kink, pre-riser cut, and post riser cut, each varying with time as the oil and gas release rate varied. The multiple trapping depths predicted by the model are consistent with extensive CDOM, BTEX, and DOSS measurements of oil and dispersant concentrations in the water column.

- The blowout plume model also clearly showed that the gas that was released during the blowout was entirely dissolved by the trap depth. Accounting for gas dissolution from the plume is important for accurate predictions of trapping depth. If dissolution is not considered the model overestimates the height of trapping. The model predictions are consistent with measurements of gas in the plume and at trapping depths.

- The blowout plume model predicted that gas concentrations in the water column did not reach saturation levels and hence hydrates were not predicted to form. This is consistent with ROV observations of the plumes from both the kink and riser and the plume trapping depth which showed no evidence of being limited by loss of buoyancy due to hydrate formation.

- The dispersant treatment model showed that the releases from the riser, both pre and post cut, rapidly transitioned from jets to buoyant plumes within a distance approximately 1 m based on the momentum length scale of the release. This is consistent with ROV observations of the kink and riser releases and independent analyses using Particle Image Velocimetry (PIV) and Acoustic Doppler Current Profiler (ADCP) methods.

- Based on ROV observations, dispersants were typically applied at the edge of the blowout plume and the dispersant entrained into the rising plume. A single wand (single opening) was principally used during the pre-cut period on the riser release, while a trident (bi-dent) (multiple openings) adjacent to the top hat, was used during the post cut period. No treatment was used on the kink releases. The multi-pronged trident impacted a significantly larger sector of the release than the wand.

- The dispersant treatment model predicts that approximately 30% of the oil released was treated during the post cut period. For the oil that was treated a dispersant chemical effectiveness of 80% was assumed. The resulting fraction treated and DOR is in reasonably good agreement when the oil droplet size distribution model is fit to Holocam observations taken during the Jack Fitz 3 cruise.

- A new empirical, unified oil droplet size model was developed, with dependence on both the Weber and Ohnesorge numbers, the latter representing viscous effects important for dispersant treated oils. The model was validated against the most recently available small and large laboratory scale experimental data and showed an excellent ability to estimate oil droplet sizes for both treated and untreated oils.

- The lognormal oil droplet size distribution function provides an excellent fit to the Holocam oil droplet data taken during the DWH spill (dives # 5 and 6) with very high R^2 values when fitted with its lognormal distribution function for all deep dives. The droplet size model is also able to account for the impact of both treated and untreated oil on the total oil droplet size predictions.

- The Holocam data (dive #5 and 6 in particular) (Davis and Loomis, 2014) support the general conclusion that oil droplets, with sizes smaller than 300 μm, remained in the water column long enough to be detected at the locations sampled (up to 2 km from the wellhead). Due to the distance of the Holocam observation from the release, droplets larger than this size are rarely observed, presumably the larger droplets having risen out of the intrusion layer due to their buoyancy.

- Predictions of the droplet size distribution are in good agreement with the limited in situ Holocam observations, clearly suggesting that the subsea dispersant application was effective in dispersing oil into the water column. Mechanically-induced dispersion of releases from the kink also played a role in dispersing oil during the pre-riser cut period.

- The fountain and intrusion model predicts a relatively thin intrusion layer that increases in thickness with distance from the source due to entrainment and is modified by the presence of ambient cross flow. The intrusion layer is consistent with observations of CDOM, BTEX, and DOSS in the water column at the plume trapping depth.

- A series of simulations using the dispersant treatment and droplet size model, with a focus on oil that is dispersed and remains in the water column, shows that even if there is no treatment, 9% of the oil is dispersed mechanically by the very energetic kink flow and to a much more limited extent the pre-cut riser flow. The present estimates assume that all droplets initially less than 300 μm are considered to be in the intrusion layer and close to the source (< 2 km). For the low, best-estimate, and high efficiency dispersant treatment cases, the amount dispersed at depth was predicted to be 11, 22, and 36%, respectively.

- To validate these results, estimates were made of the amount of oil retained in the intrusion layer using the results of the fountain and blowout plume model predictions of the flow rates in the intrusion layer, and BTEX (components of the source oil) and DOSS (a component of dispersants) measurements at the trapping depth. The model estimates that 27% ± 5% of the BTEX and 90% ± 23% of the DOSS were retained in the intrusion layer (based on post cut analysis only). The very high level of retention of DOSS is consistent with the idea that dispersant and dispersant treated oil is primarily retained in the intrusion layer. Estimates from the Oil Budget Calculator (OBC) for retention of both chemically and mechanically dispersed oil ranged from 20 to 38%, with an expected value of 25%. Estimates from hydrocarbon chemistry ranged from 28 to 45%, with an average value of 36%. Predictions from the present simulations (8 to 33 %, with a best estimate of 20%) are in good agreement with the various independent estimates, in terms of both the mean values, as well as the range.

6. References

Anderson, K., G. Bhatnagar, D. Crosby, G. Hatton, P. Manfield, A. Kuzmicki, N. Fenwick, J. Pontaza, M. Wicks, S. Socolofsky, C. Brady, S. Svedeman, A. K. Sum, C. Koh, J. Levine, R. P. Warzinski and F. Shaffer. 2012. Hydrates in the ocean beneath, around, and above production equipment. Energy & Fuels 26(7):4167-4176.

Ansong, J, P. J. Kyba, and B. R. Sutherland, 2008. Fountains impinging on a density interface, J. Fluid Mech. (2008), vol. 595, pp. 115–139. c 2008 Cambridge University Press

Belore, R. 2014. Subsea chemical dispersant research. Proceedings of The 37th AMOP Technical Seminar on Environmental Contamination and Response, Environment Canada, Canmore, Alberta, Canada. Pp. 618-650.

Brandvik, P. J., Ø. Johansen, U. Farooq, G. Angell and F. Leirvik. 2014. Sub-surface oil releases – Experimental study of droplet distributions and different dispersant injection techniques-version 2. A scaled experimental approach using the SINTEF Tower basin. SINTEF report no: A26122. Trondheim Norway 2014. ISBN: 9788214057393.

BP,2010. GoM Dilling, Completions and Interventions – Mc252, Guidance on Subsea Dispersant Application, Ops note #4. Round 6, Procedure's folder, pp. 298-307,2200-T2-DO-PR-4453-0.

Bushnell, N., 2013. Oil spill by the oil rig "Deepwater Horizon" in the Gulf of Mexico – capping stack flow calculations, July 12 to 15, 2010, Expert report in matter of US vs BP Exploration & Production, Inc. et al, submitted to the US Department of Justice, March 22, 2013.

Camilli R., Di Iorio D., Bowen A., et al., 2011. Acoustic measurement of the Deepwater Horizon Macondo well flow rate, Proceedings of the National Academy of Sciences. www.pnas.org/cgi/doi/10.1073/pnas.1100385108

Chan, G. K. Y., A. C. Chow and E. E. Adams. 2014. Effects of droplet size on intrusion of sub-surface oil spills. Environmental Fluid Mechanics 14(5):1-15.

Davis, C. S. and N. C. Loomis. 2014. Deepwater Horizon Oil Spill (DWHOS) Water Column Technical Working Group, Image Data Processing Plan: Holocam description of data processing methods used to determine oil droplet size distributions from in situ holographic imaging during June 2010 on cruise M/V Jack Fitz 3. Woods Hole Oceanographic Institution and MIT/WHOI Joint Program in Oceanography. 15 pages + Appendices.

Delvigne, G. a. L. and C. E. Sweeney, 1988. Natural dispersion of oil. Oil and Chemical Pollution 4(4):281-310.

Delvigne, G. a. L. and L. J. M. Hulsen, 1994. Simplified laboratory measurement of oil dispersion coefficient - Application in computations of natural oil dispersion. Proceedings of the Seventeenth Arctic and Marine Oil Spill Program (AMOP) Technical Seminar, Vancouver, B.C., Environmental Protection Service, Environment Canada, pp.173-187.

Dykhuizen, R. C., 2013. Flow rates from the Macondo MC252 well, Expert report in matter of US vs BP Exploration & Production, Inc. et al, submitted to the US Department of Justice, March 22, 2013.

French McCay, D., K. Jayko, Z. Li, M. Horn, Y. Kim, T. Isaji, D. Crowley, M. Spaulding, J. Fontenault, R. Shmookler and J. Rowe. 2015. Technical Reports for Deepwater Horizon Water Column Injury Assessment, WC_TR.14: Modeling oil fate and exposure concentrations in the Deepwater plume and rising oil resulting from the Deepwater Horizon Oil Spill. September 08, 2015; Project No, 2011-144. RPS ASA, 55 Village Square Drive, South Kingstown, RI 02879

French McCay, D.P, Z. Li, M. Horn, D. Crowley, M. Spaulding, D. Mendelsohn, and C. Turner, 2016. Modeling Oil Fate and Subsurface Exposure Concentrations from the Deepwater Horizon Oil Spill. pp. 115-150 In: Proceedings of the 39th AMOP Technical Seminar on Environmental Contamination and Response, Emergencies Science Division, Environment Canada, Ottawa, ON, Canada.

French McCay, D., M. Horn, Z. Li, D. Crowley, M. Spaulding, D. Mendelsohn, K. Jayko, Y. Kim, T. Isaji, J. Fontenault, R. Shmookler, and J. Rowe. 2017. Simulation Modeling of Ocean Circulation and Oil Spills in the Gulf of Mexico – Appendix VI Data Collection, Analysis and

Model Validation. Prepared by RPS ASA for the US Department of the Interior, Bureau of Ocean Energy Management, Gulf of Mexico OCS Region, New Orleans, LA. OCS Study BOEM 2017.

Grennan, M., S. Zamorski, L. Decker, M. Horn, and Y. Kim, 2015. Technical Reports for Deepwater Horizon Water Column Injury Assessment – FE_TR.39: Volume II. Water column CTD and sensor data from the Deepwater Horizon oil spill. RPS ASA, South Kingstown, RI, USA, August 2015.

Griffith, S. K., 2013. Oil release from the Macondo MC252 well, Expert report in matter of US vs BP Exploration & Production, Inc. et al, submitted to the US Department of Justice, March 22, 2013.

Hinze, J. O. 1955. Fundamentals of the hydrodynamic mechanism of splitting in dispersion processes. Journal of AICHE 1:289-295.

Horn, M., D. French McCay, J. Payne, W. Driskell, Z. Li, M. Grennan, L. Decker, S. Zamorski, 2015. Technical Reports for Deepwater Horizon Water Column Injury Assessment –Volume III. Water Column Chemical and Physical Data from the Deep Water Horizon Blowout. RPS ASA, South Kingstown, RI, USA, August 2015. DWH-AR0024617.pdf [https://www.doi.gov/deepwaterhorizon/adminrecord]

Johansen, Ø., Rye, H., Melbye, A.G., Jensen, H.V., Serigstad, B., Knutsen, T., 2001. DeepSpill JIP—Experimental discharges of gas and oil at Helland Hansen—June 2000. Technical Report, SINTEF Report STF66 F01082, SINTEF Applied Chemistry, Trondheim, Norway, p. 159.

Johansen, Ø., et al. 2001. Deep Spill JIP – Experimental discharges of gas and oil at Helland Hansen – June 2000. SINTEF, Final Technical Report.

Johansen, Ø., P. J. Brandvik and U. Farooq, 2013. Droplet breakup in subsea oil releases – Part 2: Predictions of droplet size distributions, with and without injection of chemical dispersants. Marine Pollution Bulletin 73(1):327-335.

Kelkar, M. and R. Raghavan, 2013. Rate prediction from the Macondo well, Expert report in matter of US vs BP Exploration & Production, Inc. et al, submitted to the US Department of Justice, March 22, 2013.

Kessler J.D., Valentine D.L., Redmond M.C., Du M., Chan E.W., Mendes S.D., Quiroz E.W., Villanueva C.J., Shusta S.S., Werra L.M., Yvon-Lewis S.A., and Weber T.C. 2011. A persistent oxygen anomaly reveals the fate of spilled methane in the deep Gulf of Mexico. Science 331: 312-315.

Kujawinski, E.B., M. C. K. Soule, D. L. Valentine, A. K. Boysen, K. Longnecker, and M. C. Redmond, 2011. Fate of dispersants associated with the Deepwater Horizon oil spill. Environ. Sci. & Technol., American Chemical Society Publications. American Chemical Society, 2011

Lehr, B., S. Bristol and A. Possolo, 2010. Deepwater horizon oil budget calculator: A report to the national incident command. The Federal Interagency Solutions Group, Oil Budget Calculator

Science and Engineering Team. http://www.restorethegulf.gov/sites/default/files/documents/pdf/OilBudgetCalc_Full_HQ-Print_111110.pdf (Accessed on April 1, 2012).

Li, Z., M. L. Spaulding, D. French McCay, D. Crowley, and J. R. Payne. 2016. Development of a unified oil droplet size distribution model with application to surface breaking waves and subsea blowout releases considering dispersant effects, Marine Pollution Bulletin http://dx.doi.org/10.1016/j.marpolbul.2016.09.008.

McNutt, M, R. Camilli, G. Guthrie, P. Hsieh, V. Labson, B. Lehr, D. Maclay, A. Ratzel, and M. Sogge. 2011. Assessment of flow rate estimates for the Deepwater Horizon / Macondo Well oil spill. Flow Rate Technical Group report to the National Incident Command, Interagency Solutions Group, March 10, 2011.McNutt MK, Camilli R, Crone TJ, et al., 2011. Review of flow rate estimates of the Deepwater Horizon oil spill. Proceedings of the National Academy of Sciences.

Payne, J.R., and W.B. Driskell, 2015a. 2010 DWH Offshore Water Column Samples—Forensic Assessments and Oil Exposures, PECI Technical Report to the Trustees in support of the pDARP. DWH-AR0039118.pdf, 2015a. [https://www.doi.gov/deepwaterhorizon/adminrecord]

Payne, J.R., and W.B. Driskell,2015b. Forensic Fingerprinting Methods and Classification of DWH Offshore Water Samples. PECI Technical Report to the Trustees in support of the pDARP, DWH-AR0039170.pdf. [https://www.doi.gov/deepwaterhorizon/adminrecord]

Pooladi-Darvish, 2013. Estimate of cumulative volume of oil released from the MC252 Macondo well. Rebuttal expert report US v BP Exploration & Production, Inc. et al. TREX-011654R. http://www.mdl2179trialdocs.com/releases/release201311071200013/TREX-011654R.PDF

Reddy, C. M., J. S. Arey, J. S. Seewald, S. P. Sylva, K. L. Lemkau, R. K. Nelson, M. a. S. Van Mooy and R. Camilli, 2012. Composition and fate of gas and oil released to the water column during the Deepwater Horizon oil spill. Proceedings of National Academy of Sciences 109(5):20229-20234.

Reed M, O.Johansen, F. Leirvik, and B. Brors, 2009. Numerical algorithm to compute the effects of breaking waves on surface oil spilled at sea. Final report submitted to NOAA/UNH Coastal Response Research Center. Vol. 19 + appendices. SINTEF Institute for Materials and Chemistry.

Ryerson T. B., R. Camilli, J. D. Kessler, E. B. Kujawinski , C. M. Reddy, D. L. Valentine, E. Atlas, D. R. Blake, J. de Gouwa, S. Meinardi, D. D. Parrish, J. Peischl, J. S. Seewald, and C. Warneke, 2012. Chemical data quantify Deepwater Horizon hydrocarbon flow rate and environmental distribution, Proceedings of the National Academy of Sciences, www.pnas.org/cgi/doi/10.1073/pnas.1110564109

Socolofsky, S. A., E. E. Adams, and C. R. Sherwood. 2011. Formation dynamics of subsurface hydrocarbon intrusions following the Deepwater Horizon blowout. Geophys. Res. Lett. 38(9): L09602. doi:10.1029/2011GL047174

Spaulding, M. L., P.R. Bishnoi, E. Anderson, and T. Isaji, 2000. An integrated model for prediction of oil transport from a deep water blowout, 23 rd Arctic and Marine Oil Spill Program (AMOP) Technical Seminar, June 14-16, 2000, Vancouver, British Columbia, Canada, pp.611-636.

Spaulding, M.L., Mendelsohn, D., Crowley, D., Li, Z., Bird, A., 2015. Draft Technical Reports for Deepwater Horizon Water Column Injury Assessment: Application of OILMAP DEEP to the Deepwater Horizon blowout. Prepared for National Oceanic and Atmospheric Administration (NOAA) by RPS ASA, South Kingstown, RI, U.S.A. September 29, 2015. Administrative Record No. DWH-AR0285366. Available online, https://www.doi.gov/deepwaterhorizon/adminrecord and specifically at https://www.fws.gov/doiddata/dwh-ar-documents/830/DWH-AR0285366.pdf.

Spier, C., W. T. Stringfellow, T. C. Hazen, and M. Conrad, 2013. Distribution of hydrocarbons released during the 2010 MC252 oil spill in deep offshore waters, Environmental Pollution, 173, 224-230.

US Coast Guard(USCG), 2010. DH Riser Kink Holes - Measurements with field drawing and images. U.S Coast Guard - Research & Development Center, Groton, CT.

USDC, 2015. The US District Court for Eastern District of Louisiana, Case 2:10-md-02179-CJB-SS Document 14021 Filed 01/15/15, Findings of fact and conclusions of law phase two trial. Pp 1-44. (http://www2.epa.gov/sites/production/files/2015-01/documents/phase2ruling.pdf)

Van Wylen, G. J. and R. E. Sontag, 1973. *Fundamentals of Classical Thermodynamics*, Wiley and Sons

Venkataraman, P., J. Tang, E. Frenkel, G. L. Mcpherson, J. He, S. R. Raghavan, V. L. Kolesnichenko, A. Bose and V. T. John. 2013. Attachment of a hydrophobically modified biopolymer at the oil-water interface in the treatment of oil spills. Applied Materials & Interfaces 5(9):3572-3580.

Wereley, S., 2011. Gulf oil spill Particle Image Velocimetry (PIV) analysis, Appendix 5, Appendix D Plume Calculation Team, PIV report, from McNutt M., R. Camilli,G. Guthrie G, et al. 2011. Assessment of flow rate estimates for the Deepwater Horizon / Macondo Well oil spill. Flow Rate Technical Group report to the National Incident Command, Interagency Solutions Group, March 10, 2011.

Zick, A. 2013. Equation of state fluid characterization and analysis of the Macondo reservoir fluids, Expert report in matter of US vs BP Exploration & Production, Inc. et al, submitted to the US Department of Justice, March 22, 2013.

Acknowledgements:

Funding of this research was provided by the Federal and State Natural Resource Agencies' (Trustees') Natural Resource Damage Assessment (NRDA) for the DWH oil spill through the National Oceanic and Atmospheric Administration Damage Assessment, Remediation and Restoration Program (NOAA Contract No. AB133C-11-CQ-0050). The opinions expressed by the authors are their own and do not necessarily reflect the opinion or policy of the U.S. Government. Any use of trade, firm, or product names is for descriptive purposes only and does not imply endorsement by the U.S. Government. The authors extend thanks to Scott Socolofsky, Texas A&M, College Station, TX for his in depth review of the technical report upon which this paper is based and to various reviewers from the NOAA NRDA program.

Acronyms:

ADCP- Acoustic Doppler Current Profiler

AMOP - Arctic Marine Oil spill Program

BP - British Petroleum

BTEX - Benzene, Toluene, Ethylbezene, and o-, m-, and p-Xylene

BOP- blowout preventer

BOT- Black Oil Tables

CDOM - Colored Dissolved Organic Matter

CTD - conductivity, temperature, and depth

DARP - Damage Assessment, Remediation and Restoration Program

DOR - dispersant to oil ratio

DOSS - dioctyl sodium sulfosuccinate

DWH - Deep Water Horizon spill

FRTG - Flow Rate Technical Group

JF - Jack Fitz Cruise

NOAA - National Oceanic and Atmospheric Administration

NRDA - Natural Resource Damage Assessment

OBC - oil budget calculator

Oh - Ohnesorge number

OILMAP DEEP - integrated oil blowout modeling system

PIV - particle image velocimetry

ROV - remotely operated vehicle

SIMAP - 3D oil spill transport and fate model

USCG - US Coast Guard

USDC - US District Court

VMD - volume median diameter

We - Weber number

Table 1. **Cumulative (volume) oil droplet size distribution for no dispersant treatment and low, best-estimate, and high treatment cases. The values for 300 µm, the presumed trap depth size, are highlighted.**

Droplet Size	Dispersant Treatment			
µm	None	Low	Best-estimate	High
100	0.01	0.01	0.07	0.03
200	0.05	0.06	0.17	0.20
300	0.09	0.11	0.22	0.36
400	0.11	0.16	0.25	0.47
500	0.12	0.21	0.26	0.54
1000	0.20	0.47	0.32	0.69
2000	0.53	0.75	0.60	0.83
5000	0.95	0.98	0.96	0.98
10000	1.00	1.00	1.00	1.00

Table 2 **Estimates of the percent oil dispersed into the deep water from various sources (Spaulding et al, 2015)**

	Source	Percent Oil Dispersed (%)
	OILMAP DEEP predictions	No treatment - 6, low -8, best estimate-20, high treatment -33
	Data Based Estimates	
1	Fountain and intrusion model with entrainment and BTEX data	27 ± 5 post cut
2	Oil Budget Calculator (mechanically and chemically dispersed subsurface)(Lehr et al, 2010)	low - 20, expected-25, and high-38
3	Oil Budget Calculator (only chemically dispersed subsurface)(Lehr et al, 2010)	low -9, expected -14, and high -27
4	Hydrocarbon chemistry (Ryerson et al, 2012)	low – 28, average – 36, and high - 45
	Range of Estimates	9 to 45
	Average of Estimates	25.5

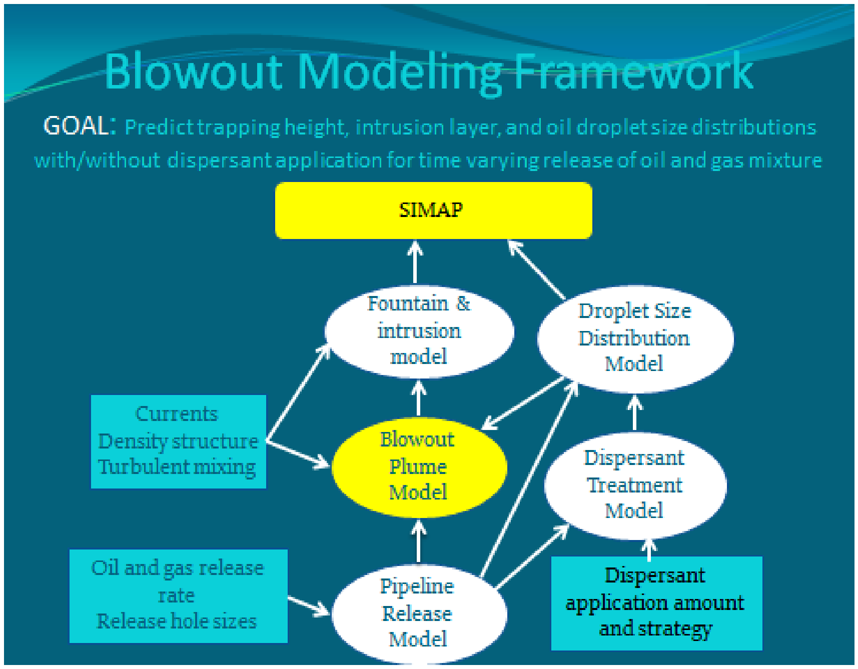

Figure 1. **Overview of OILMAP DEEP integrated blowout model system. Ovals show individual model components and boxes show the required environmental, oil and gas release, and dispersant application data. The blowout plume model is highlighted in yellow as it is the core of OILMAP DEEP. The blowout plume model provides input to the fountain and intrusion model, which in turn provides information on the vertical extent of the intrusion layer where oil droplets are initially placed for the subsequent far field modeling in SIMAP.**

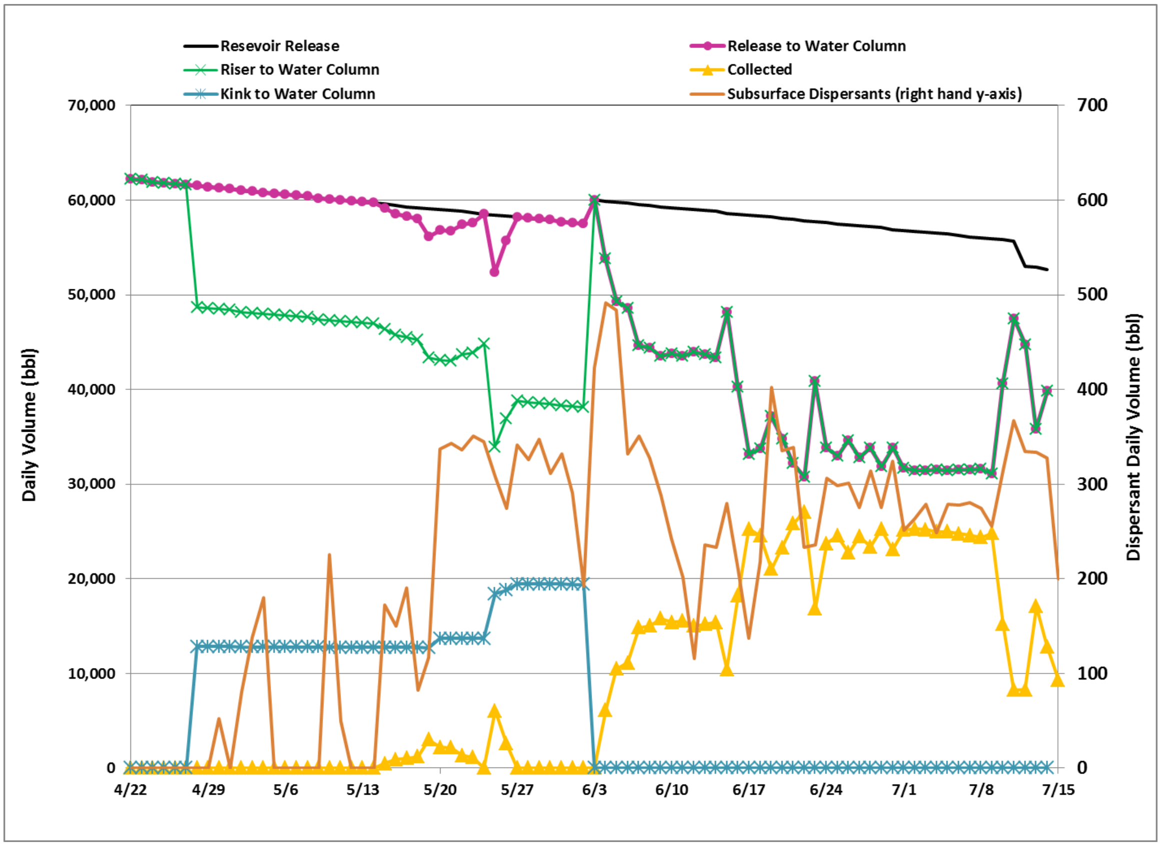

Figure 2. **Time history of the estimated total oil release rate based on the Oil Budget Calculator (OBC) (Lehr et al. 2010), with and without adjustment for the amount recovered via the top hat installed on June 3, 2010. Estimates of the oil release rates from reservoir, riser, and kink are provided. The amount of oil recovered and released to the water column is also given (reservoir minus amount collected). The amount of dispersants applied subsurface to the spill is also provided. All rates are in barrels per day.**

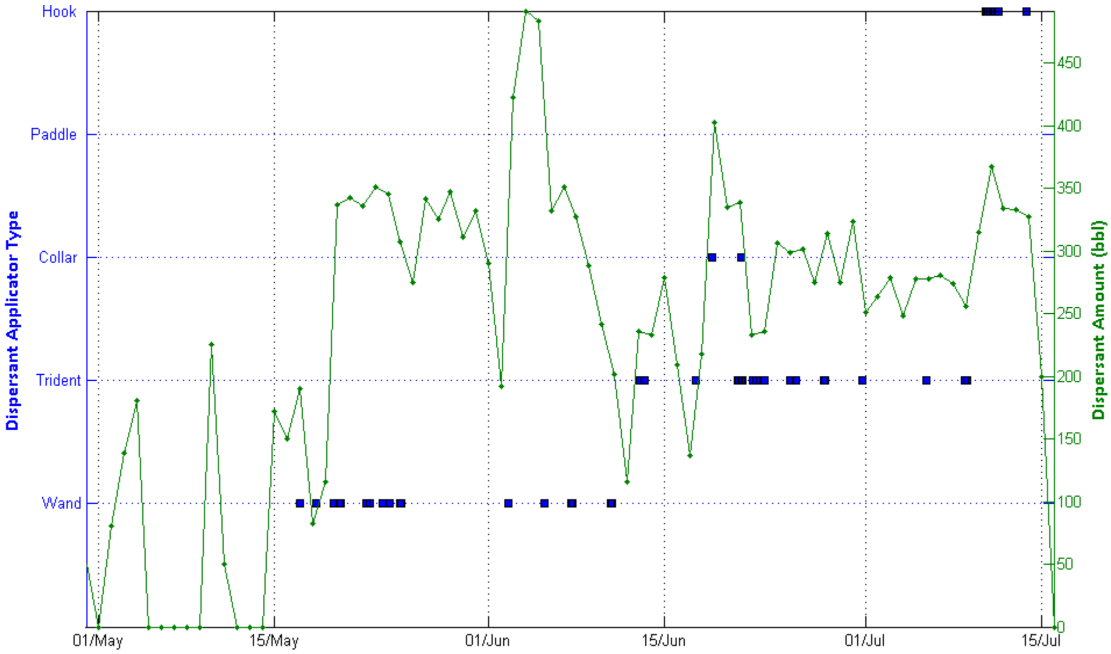

Figure 3. **Dispersant applicator time series, showing observed presence of dispersant application method from sampled ROV video (left axis, when known), and subsea dispersant amounts in barrels (right axis). The riser cutting operation was performed between May 31 and June 3, 2010.**

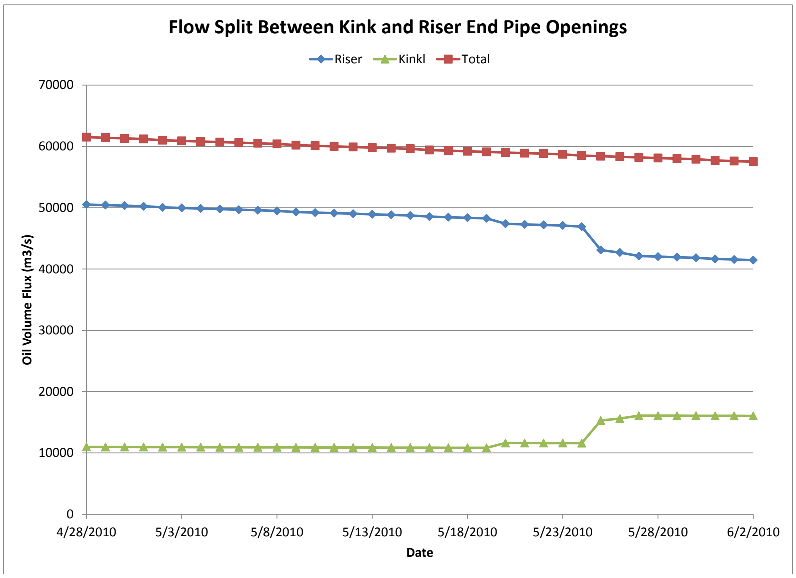

Figure 4 **Pipeline release model predicted flow spilt between the kink holes and the riser outlet**

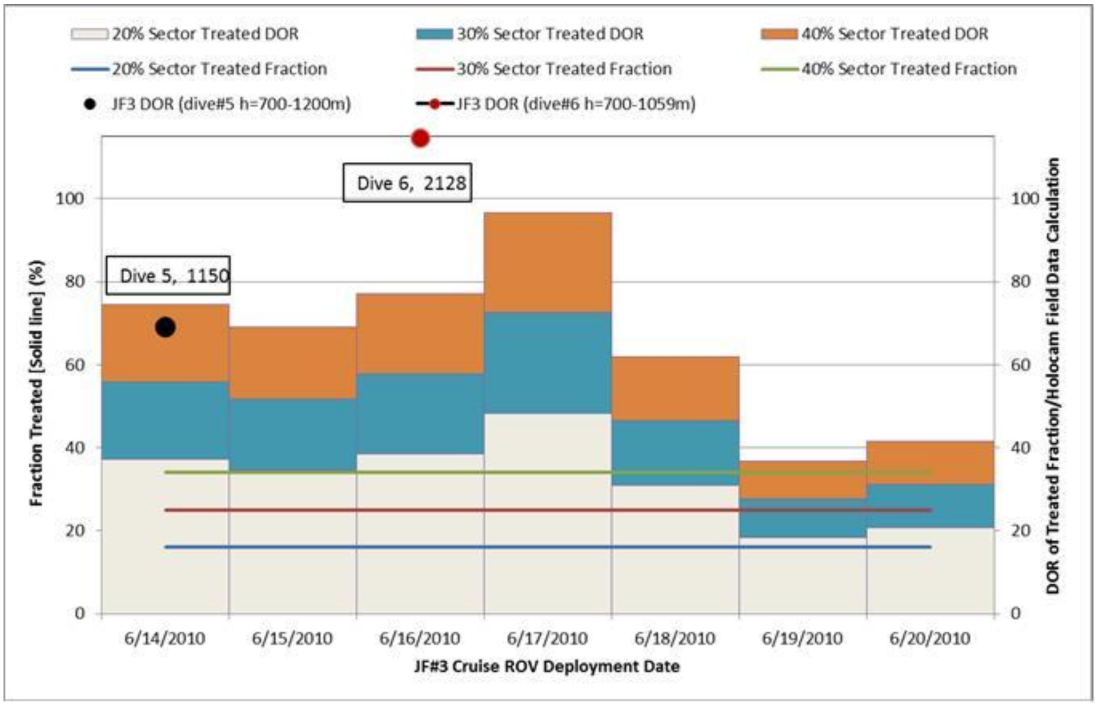

Figure 5. **Fraction treated (blue, red, and green solid line, left axis) and DOR (stacked columns, right axis) during the JF3 cruise for sectors treated 20%, 30%, and 40%, respectively. The estimated/modeled DORs for the JF3 dives are also plotted (filled circles) along with the dive number and the distance (m) from the wellhead.**

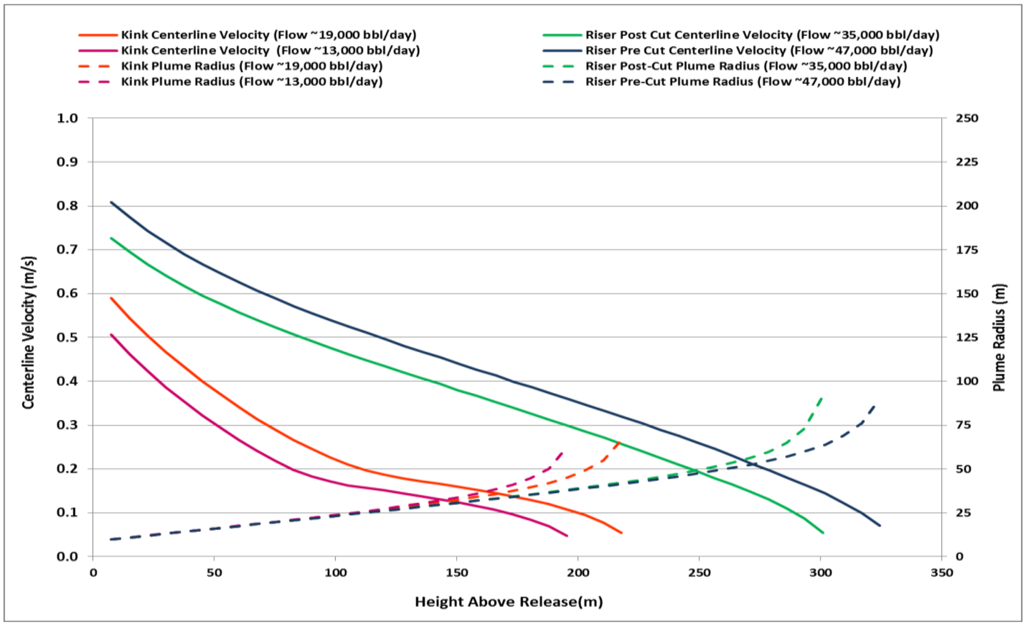

Figure 6. **Plume radius and centerline velocities for typical conditions for pre- and post-cut of the riser releases and the kink release.**

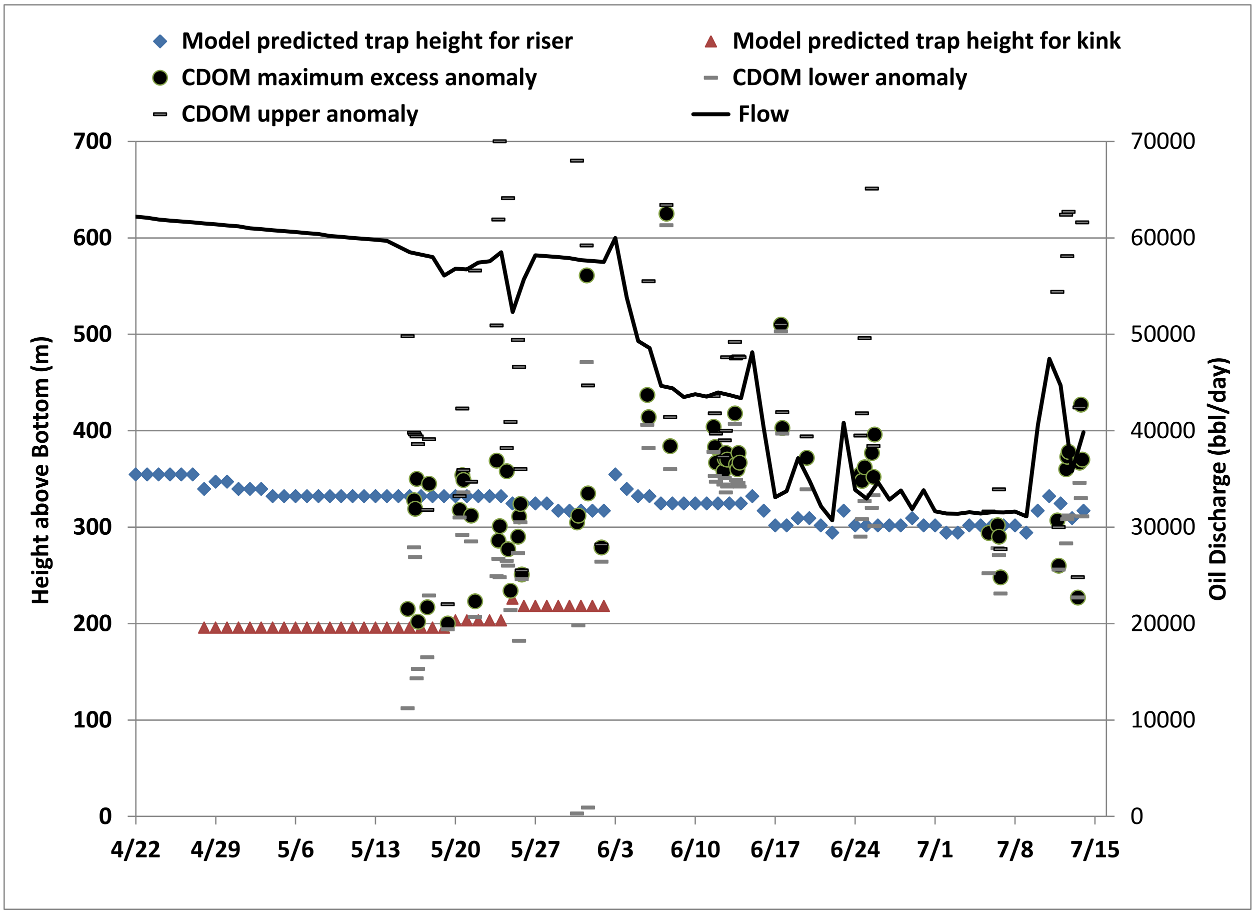

Figure 7. **Model predicted trap height vs. observed CDOM anomaly (Horn et al, 2015).**

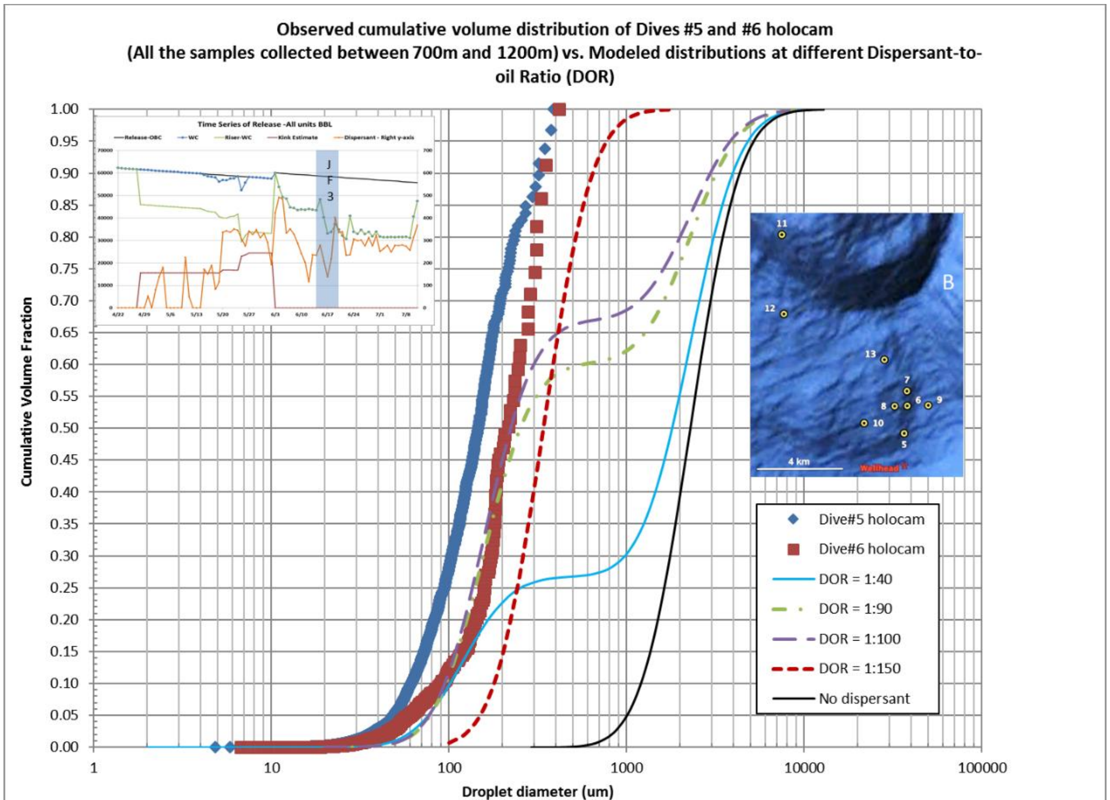
Observed cumulative volume distribution of Dives #5 and #6 holocam
(All the samples collected between 700m and 1200m) vs. Modeled distributions at different Dispersant-to-oil Ratio (DOR)
Cumulative Volume Fraction
Droplet diameter (um)
Time Series of Release -All units BBL
Release-OBC
WC
Riser-WC
Kink Estimate
Dispersant - Right y-axis
J
F
3
11
12
13
7
8
6
9
10
5
B
4 km
Wellhead
Dive#5 holocam
Dive#6 holocam
DOR = 1:40
DOR = 1:90
DOR = 1:100
DOR = 1:150
No dispersant

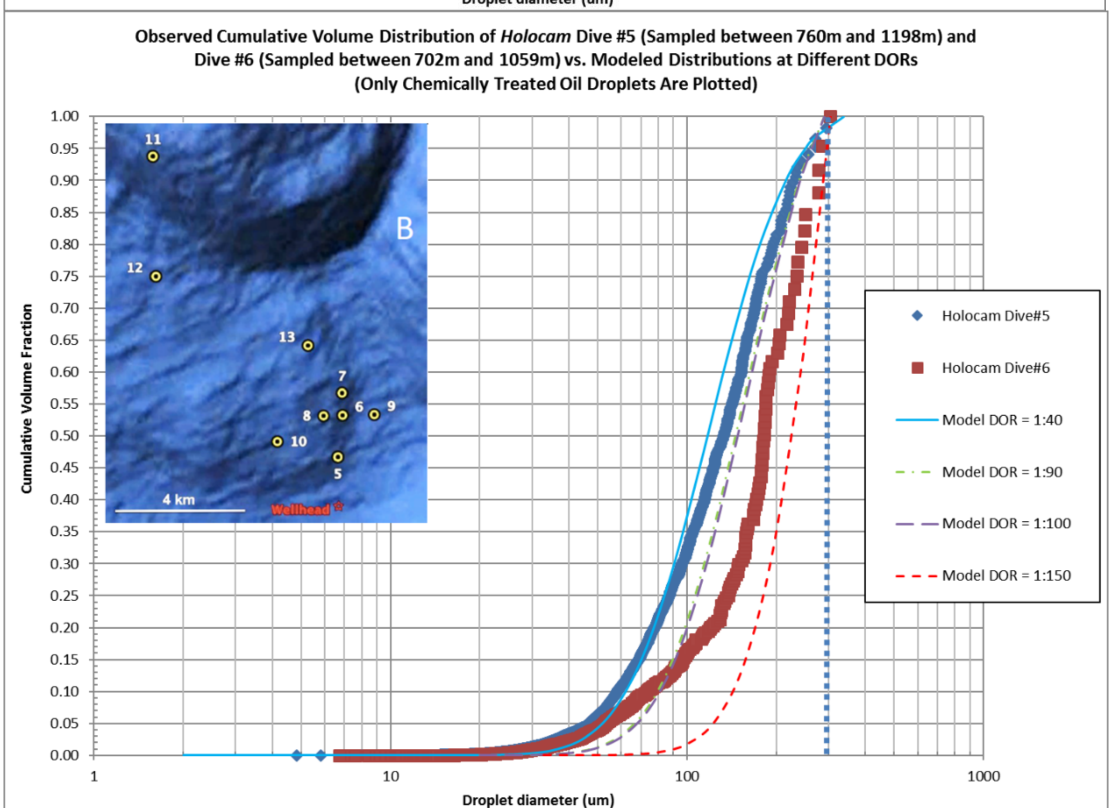
Observed Cumulative Volume Distribution of Holocam Dive #5 (Sampled between 760m and 1198m) and Dive #6 (Sampled between 702m and 1059m) vs. Modeled Distributions at Different DORs
(Only Chemically Treated Oil Droplets Are Plotted)
Cumulative Volume Fraction
Droplet diameter (um)
11
12
13
7
8
6
9
10
5
B
4 km
Wellhead
Holocam Dive#5
Holocam Dive#6
Model DOR = 1:40
Model DOR = 1:90
Model DOR = 1:100
Model DOR = 1:150

Figure 8 **Comparison of the observed oil droplets cumulative volume size distribution and the predicted cumulative volume size distribution for four different DORs and assuming no dispersant effectiveness. The observational data are from the two dives (#5 and #6) that were reported to have much oil in deep water (Davis and Loomis, 2014) of the M/V JF3 cruises during June 14-20, 2010. Top panel: The model distributions are the compound distributions of the chemically and physically (non-treated) dispersed oil droplets, based on an average daily release rate of 38,700 bbls oil to the water column, and a dispersant application rate of 259 bbls Corexit 9500 per day. Dispersant effectiveness was assumed 100% at various simulated DORs, or 0% for the no-dispersant model. Lower panel: The model distributions are presented for the dispersed fraction of oil droplets d ≤ 300 μm only, recalculated to be cumulative to 300 μm; Dotted line in the lower panel highlights the 300 μm cut-off size.**

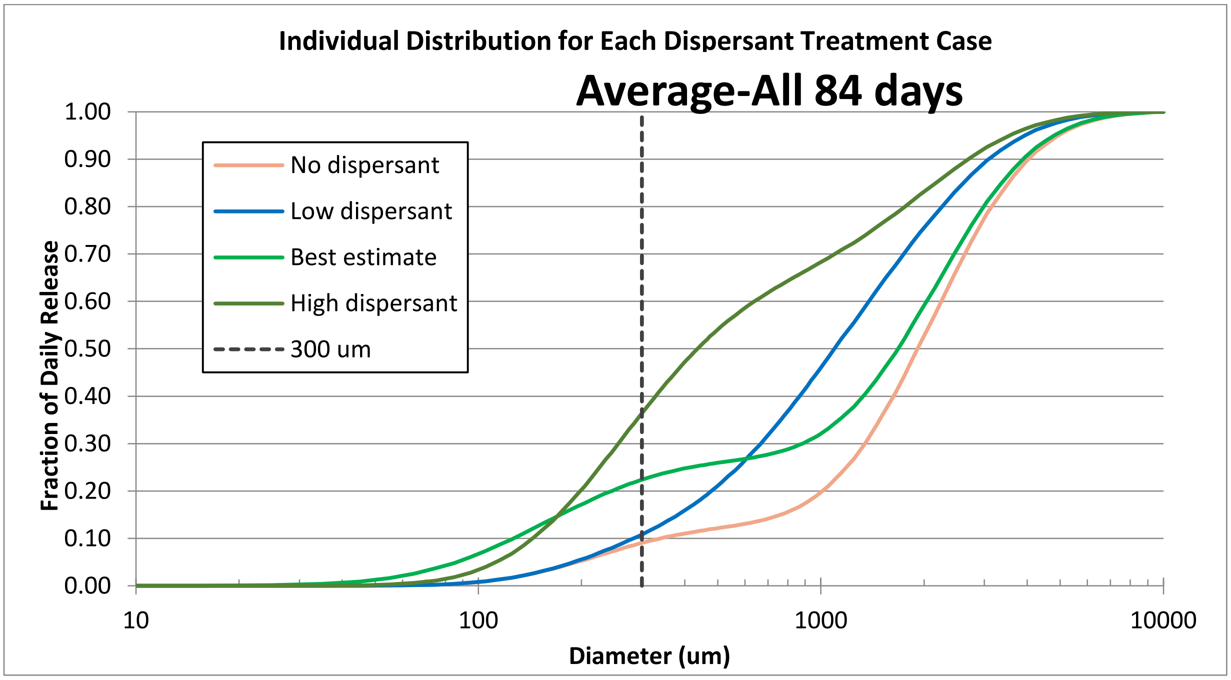

Individual Distribution for Each Dispersant Treatment Case
Average-All 84 days
No dispersant
Low dispersant
Best estimate
High dispersant
300 um
Fraction of Daily Release
1.00
0.90
0.80
0.70
0.60
0.50
0.40
0.30
0.20
0.10
0.00
10
100
1000
10000
Diameter (um)

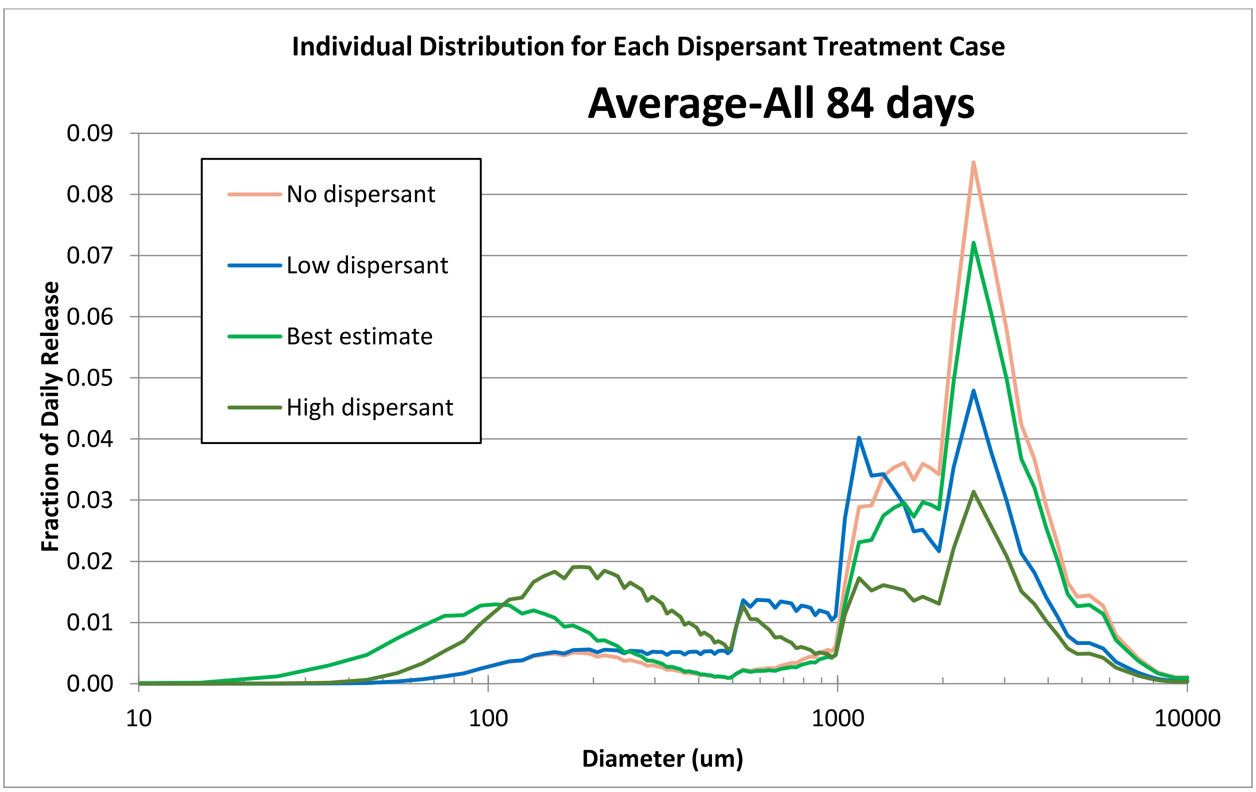

Individual Distribution for Each Dispersant Treatment Case
Average-All 84 days
No dispersant
Low dispersant
Best estimate
High dispersant
Fraction of Daily Release
0.09
0.08
0.07
0.06
0.05
0.04
0.03
0.02
0.01
0.00
10
100
1000
10000
Diameter (um)

Figure 9 **Oil droplet size distribution curves of the four treatment cases (no dispersant, low dispersant, best estimate, and high dispersant application) of the total oil release throughout the entire oil spill incident: (A) upper panel, cumulative distribution; dashed line indicates the cut-off size (300µm) of oil droplets trapped in the plume layer (B) lower panel, individual distributions.**